remote sensing

MDPI

Article

Forest Fire Susceptibility Zonation in Eastern India Using Statistical and Weighted Modelling Approaches

Jayshree Das [1], Susanta Mahato [2], Pawan Kumar Joshi [1,2] and Yuei-An Liou [3,*]

[1] School of Environmental Sciences, Jawaharlal Nehru University, New Delhi 110 067, India
[2] Special Centre for Disaster Research, Jawaharlal Nehru University, New Delhi 110 067, India
[3] Centre for Space and Remote Sensing Research, National Central University, Taoyuan 320317, Taiwan
* Correspondence: yueian@csrsr.ncu.edu.tw

Abstract: Recurring forest fires disturb ecological balance, impact socio-economic harmony, and raise global concern. This study implements multiple statistical and weighted modelling approaches to identify forest fire susceptibility zones in Eastern India. Six models, namely, Frequency Ratio (FR), Certainty Factor (CF), Natural Risk Factor (NRF), Bivariate statistical (Wi and Wf), Analytical Hierarchy Process (AHP), and Logistic Regression (LR) were used in the study. Forest fire inventory (2001 to 2018) mapping was done using forest fire points captured by the MODIS (Moderate Resolution Imaging Spectroradiometer) sensor. Fire responsible components, namely, topography (which has four variables), climate (5), biophysics (8) and disturbance (4) were used as inputs to the modelling approaches. Multicollinearity analysis was carried out to examine the association and remove the highly-correlated variables before performing the modeling. Validation of model prediction levels was done using Area Under the Receiver Operating Characteristic Curve (ROC curve-AUC) value. The results reveal that the areas with west and southwest orientations, and moderate slope demarcate higher susceptibility to forest fire. High precipitation areas with lower temperature but ample solar radiation increase their susceptibility to forest fire. Mixed deciduous forest type with ample solar radiation, higher NDVI, lower NDWI and lower TWI values exhibits higher susceptibility. Model validation shows that LR (with AUC = 0.809) outperforms other models used in the study. To minimize the risk of fire and frame with proper management plans for the study area, susceptibility mapping using satellite imageries, GIS technique, and modelling approaches is highly recommended.

Keywords: forest fire susceptibility; spatial mapping; statistical modelling; prediction; validation

Citation: Das, J.; Mahato, S.; Joshi, P.K.; Liou, Y.-A. Forest Fire Susceptibility Zonation in Eastern India Using Statistical and Weighted Modelling Approaches. *Remote Sens.* **2023**, *15*, 1340. https://doi.org/10.3390/rs15051340

Academic Editor: Luke Wallace

Received: 1 January 2023
Revised: 20 February 2023
Accepted: 23 February 2023
Published: 27 February 2023

1. Introduction

Globally, fires are a recurring event in forests [1], resulting in global ecological impact [2] and local to regional socio-economic challenges [3]. In addition, they are an important agent for changing the pattern of forest composition and structure [4,5] and environmental hazards resulting in negative impacts on atmosphere, infrastructure, and human well-being [6–9]. In the Indian context, black carbon emissions from forest fires alter the surface albedo and increase snow melt from the Himalayan mountains [10]. Forest managers, climate modelers, policy makers, and the scientific community are interested in forest fire susceptibility mapping [11] through an evidence-based approach to explain the fatal consequences of fire [3] and future scenarios of fire prone environments [12]. Such information is much needed in contemporary times, as it regulates negative consequences on potentially affected groups and helps conservation and restoration activity [6,13]. This supports the respective agencies in resource distribution, early warning systems, emergency services, and forest management and planning [4]. Hence, the prediction of forest fire susceptibility with better accuracy and enhancement of fire mitigation plans are a priority in order to enhance sustainable development.

This need has been brought about by the development of various prediction models, which have focused on explaining spatio-temporal patterns that relate different components (topography, climate, biophysics and disturbances) with ignition arson wildfires [12]. The Geographical Information System (GIS) provides means to manipulate spatial information on the components that contribute to forest fire occurrence for generations on the forest fire susceptibility map [14]. Alcasena et al. [15] studied the optimization of prescribed fire allocations (climate, fuel availability) for designing fire resilient ecosystems using a geospatial database. Assessing forest fire hazard, susceptibility, and risk mapping are feasible with the geospatial techniques used by such researchers as Pourghasemi et al., Adab et al., and Eugenio et al. [16–18], and as this can improve management plans [18], minimize spread, and reduce the frequency of fire.

To study the complexity of forest fires, various modelling approaches have been anticipated. Researchers classified fire models into three categories: (i) the physically-based model, which necessitates detailed and highly accurate data for prediction of spatio-temporal pattern of forest fire; (ii) the semi-empirical model that requires several laboratory experiments; and (iii) empirical modelling that relies on the analysis of fire responsible variables using statistical and data mining methods [19]. Empirical modelling is based on the study of local environmental factors influencing forest fire ignition and spread and explains the importance of each factor in the prediction of responsible variables. It provides predictions of future fires and demarcates highly susceptible zones. Researchers support the use of the statistical modelling approach in combination with GIS technology, which covers vast forest areas and helps with the accessibility and handling of spatial data of large regions [4,20]. Boubeta et al. [12] presented spatial patterns of forest fire modelling in relation to biophysical and human variables using multiple regressions. Various approaches used by researchers for the analysis of forest fire susceptibility mapping and probability distribution are the evidential belief function model [8], the modified Analytical Hierarchy Process (AHP), and the Mamdani fuzzy logic models [16], AHP [18], area level Poisson mixed modelling [12], fuzzy AHP, the Dong model [6], and the regression model that explains drivers of forest fires [10]. Modelling approaches used in the prediction of fire hazards proved to produce better results in the delineation of forest fire prone locations and the development of explicit hazard mitigation plans by taking advantage of remote sensing and GIS techniques [8].

Fire igniting components change with the spatial and temporal extents of varying regions. It is difficult to identify fire stimulating components, which make analysis of behavior of fire a challenging task [2]. The factors intensifying large fires are increasing temperature [21], accumulating fuel load [1,22], buildup fire conquest policies, lack of management, rural flight and extensive afforestation [15]. In the recent times, forest fire responsible environmental variables have been employed to develop susceptibility map. Forest fire ignition and spread are affected by interaction of environmental variables grouped under four main categories: topography, climate, vegetation cover, and human [6,8,9,23]. The combination of the presence of an ignition source and ample circumstance for fire spread ensue the probability of forest fire [12]. Rate and spread of forest fire changes with varying topographic features like slope, aspect, and elevation [24]. Changing climatic variables, i.e., insolation, less precipitation and long dry spell, contribute towards natural wildfire and interventions of human activities increase frequency of forest fires and reach at an alarming rate [4,5,25]. Increasing precipitation supports large biomass deposition, resulting higher fuel load and thus provoking fire susceptibility [26]. Lower precipitation and higher temperature reduce moisture content of fuel load and thus make it highly flammable but fire susceptibility increases in the zone associated with continuous availability of forest biomass [25]. Understanding the fire behavior and spread in the region needs a prior idea of relationship between existing topography, vegetation characteristics and local climate [15]. Changes in the aforementioned factors are greatly influenced by human disturbances and produce unintended consequences [20].

Understanding the factors that influence the fire occurrence and its environmental and socio-economic consequences is required for the sustainable management of forest in the eastern India. Our study aims to utilize multiple statistical and weighted modelling approaches to identify forest fire susceptible zones by spatial clustering of fire incidences with prevailing fire responsible variables. The main tasks of the study are: (i) preparation of fire inventory map, (ii) enlisting fire responsible variables, and (iii) fire susceptibility mapping using weighted or statistical modeling approach and validating prediction. The variables are supposed to reveal the effect of natural conditions in the study area, importance in fire occurrence assessment and susceptibility prediction [20]. Six different methods, namely, Frequency ratio (FR), Certainty factor (CF), Natural risk factor (NRF), Wi method, Logistic regression (LR) and Analytical hierarchy process (AHP) are used in the study to assess the susceptibility of a forest patch. The study presents the ability of models to predict forest fire susceptibility and importance of each variable classes. It demarcates variable class highly responsible for forest fire occurrence. The findings of the study can be utilised in developing early warning system, fire arrest resource designing, and task allocation for developing plans to avert forest fires and implement controls for managing actual forest fires.

The research gaps addressed in this study are the lack of comprehensive study on multiple statistical and weighted modelling approaches and analysis of forest fire susceptibility in Eastern India. Although there exist previous studies that attempted to address this issue, none of them has used all possible multiple statistical and weighted modelling approaches to determine the susceptibility zones. This makes the current study novel as it offers a more comprehensive and accurate approach to identify areas that are at high risk for forest fires. The novelty of this work lies in its focus on addressing a real-world environmental problem through applied research. By identifying the susceptibility zones, the study aims to provide practical solutions for minimizing the risk of forest fires, protecting ecosystem functionality and services, improving management strategies for better land use planning in the area. This approach is unique as it is not just focused on advancing the theoretical understanding of the issue, but also provides practical solutions that can be implemented to mitigate the impacts of forest fires on the environment and local communities. Overall, the novelty and research gap addressed by this study make it an important contribution to the field of environmental management and conservation for wellbeing of human society. The results of the study will provide valuable insights into the factors that contribute to forest fire susceptibility in Eastern India and inform strategies for reducing the risk of future fires.

2. Material and Methods

2.1. Study Area

The state of Odisha in the Eastern India was chosen; it has a surface area of 155,707 sq-kms (about 4.87 percent of total geographical area of India), located between the parallels of 17°49′ North and 22°34′ North latitudes and meridians of 81°27′ East and 87°29′ East longitudes. Along the eastern extent, it has a coastline stretch of 485 km from Balasore to Ganjam districts. The climatic condition changes throughout the year with temperature varying between 10 °C and 35 °C (the highest during April-May) and an average annual rainfall is about 1500 mm. It has a rich tropical forest cover dominating with deciduous type. According to India State of Forest Report [27], Odisha is the fourth largest state in India having forest cover of 5.81 million hectares (37.69 percent of the state geographical area) and the highest forest cover is found within 0–500 m altitudinal zone. Based on the Champion and Seth [28] classification of the Forest Types of India, forests in Odisha are categorized into four Forest Type Groups comprising of 19 Forest Types [27]. Dominant forest tree species are *Shorea robusta*, *Anogeissus latifolia*, *Terminalia tomentosa*, *Madhuca latifolia*, and *Schleichera trijuga*.

About 24.53 percent of the total forest cover of the study area is identified as highly prone to forest fire [27]. The maximum number of forest fire points were recognized in the state during 2020–2021 season (the highest in the Kandhamanl District). Wildfires in some forest patches of Odisha are a frequent problem showing increasing level of harshness.

The distribution of forest fire incidences captured through Moderate Resolution Imaging Spectroradiometer (MODIS) sensor from 2001 to 2020 used in this study are shown in Figure 1.

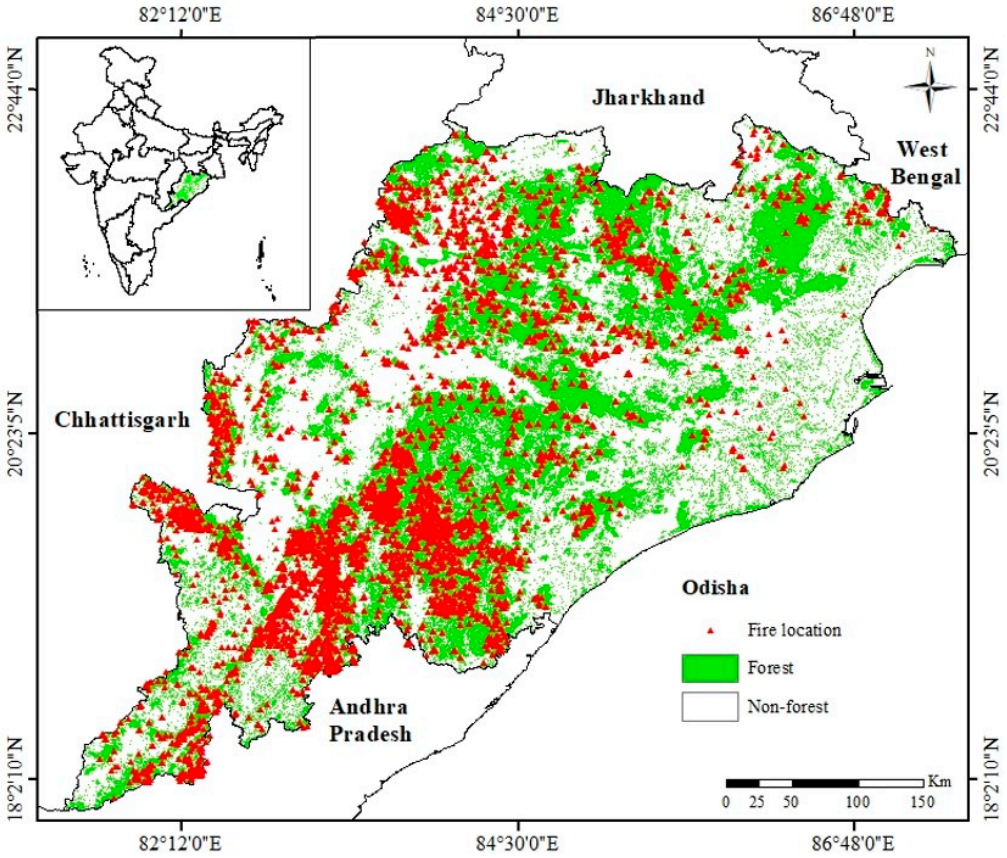

Figure 1. Study site showing forest cover and mapping forest fire inventory.

The methodology followed in the study to produce the forest fire susceptibility map is shown in Figure 2. It comprises of seven steps, (i) identify the fire locations (2001–2020) and prepare the fire inventory map, (ii) select the forest fire responsible variables and multicollinearity analysis, (iii) classify variable layers, (iv) perform weighted and statistical modeling (Frequency Ratio—FR, Certainty Factor—CF, Bivariate—Wi and Wf, Natural Risk Factor—NRF, Analytical Hierarchy Process—AHP, and Logistic Regression—LR), (v) assess variable class highly responsible for forest fire, (vi) provide forest fire susceptibility map for the study site and classify from Very High to Very Low susceptibility class, and (vii) validate models susceptibility prediction through Receiver Operator Characteristic—Area Under Curve (ROC-AUC). Computational process was carried in MS-Excel, R Studio, and SPSS Statistics 19, whereas ArcGIS 10.7.1 was used for producing susceptibility maps.

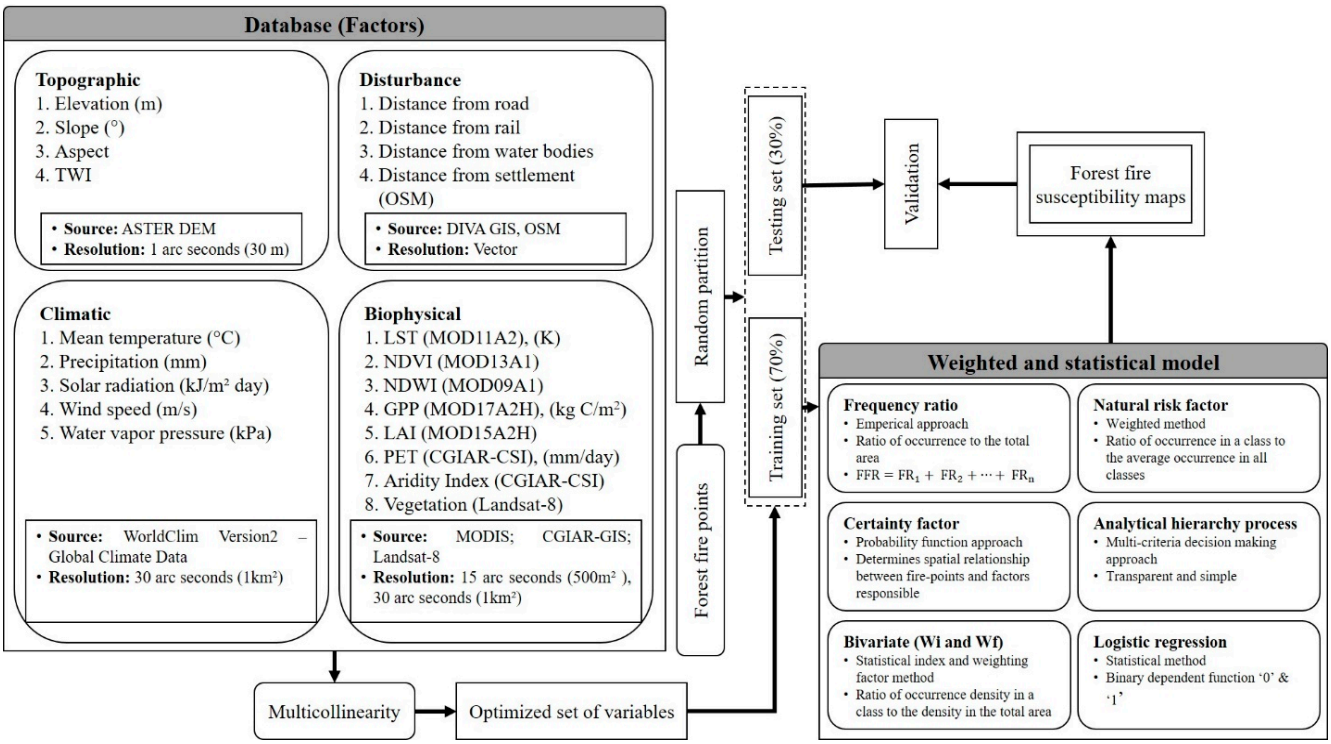

Figure 2. Flowchart showing methodology followed in the study.

2.2. Preparation of Forest Fire Inventory Map

Forest fire susceptibility prediction depends on analysis of historical forest fire locations and responsible variables leading to forest fire, which necessities preparation of fire inventory map. In this study, forest fire inventory mapping was prepared in ArcGIS from forest fire location database (MODIS sensor) provided in Forest Fire Alerts system 3.0 of the Forest Survey of India (FSI). Forest fire points were randomly split into the ratio of 70:30 as training and testing sets, respectively. Training set was used as input to models for forest fire susceptibility mapping, while accuracy assessment was done from testing set.

2.3. Forest Fire Responsible Variables

Database layers of 22 forest fire responsible variables were selected from literature review [10,16,17,29–31]. Selected variables used in the study are mentioned in Figure 2. Selection of appropriate responsible variables for forest fire susceptibility modelling is an important issue as it influence model prediction value [32]. Responsible variables include both which promote and inhibit fire, together to define the probability of forest fire in a specified spatio-temporal extent. Prior studies do not mention any fixed set of variables to be used for modelling purpose [33], whereas broadly includes topography, climate, biophysical and disturbance as components [32].

Topographic variables were obtained from the Digital Elevation Model (DEM) using Advances Spaceborne Thermal Emission and Reflection Radiometer Global Digital Elevation Map (ASTER GDEM) of 1 arc-second resolution accessed on 15 April 2022 (https://www.earthdata.nasa.gov). From DEM data slope, aspect and Topographic wetness index (TWI) were computed using ArcGIS tools.

Climate layers were prepared from database provided by WorldClim Version-2 of 30 arc-seconds resolution. It comprises of a zip file with 12 Geotiff (.tif) files, representing each month (January as 1 to December as 12). The climate components included precipitation, temperature, solar radiation, vapor pressure, and wind speed variables in the present study.

Biophysical factors comprise of Normalized Difference Vegetation Index (NDVI), Normalized Difference Water Index (NDWI), Gross Primary Productivity (GPP), Leaf Area

Index (LAI), Land Surface Temperature (LST), Potential Evapotranspiration (PET), and Aridity Index. They also make up the variables to be used for modelling approach. Landsat-8 sensor data of 1 arc-second resolution was used to define vegetation type of the study site where as data of NDVI, NDWI, LAI, LST, and GPP were collected from MODIS sensor. PET and Aridity Index (AI) data were downloaded from Consortium for Spatial Information (CGIAR-CSI) of 30 arc-seconds

Database variables comprised under disturbance like distance from road, distance from rail, distance from water bodies, and distance from settlement were obtained from Open Street Map (OSM), while Euclidean distance was computed in ArcGIS.

2.4. Multicollinearity

Multicollinearity statistics is computed to analyze the correlation between fire responsible variables [7,33] and to avoid collinearity within them [20]. Multi-collinearity is a phenomenon to predict a variable with a high degree of accuracy than other variables in the multiple regression model [20]. To quantify the severity of multicollinearity within the variables, Variance Inflation Factor (VIF) and Tolerance (TOL) were used. Although many authors adopt a tight threshold of VIF value 2 or 5, frequent rule of thumb for severe multicollinearity is employed with a threshold of 10, over which variables are considered multicollinear and eliminated from further analysis [33]. However, there are no standards for the interpretation of VIF. TOL value less than 0.1 specifies significant multicollinearity between responsible variables [34]. In this study TOL and VIF values of the variables were estimated and are given in Table 1. The highest VIF and the lowest tolerance value were 8.3 and 0.12, respectively. Therefore, to derive no multi-collinearity between responsible variables, water vapor pressure, GPP, PET, and AI were eliminated due to higher VIF value.

Table 1. Multicollinearity statistics computed for responsible variables.

Variables	Collinearity Statistics		Variables	Collinearity Statistics	
	VIF	TOL		VIF	TOL
Elevation	2.57	0.39	LAI	1.14	0.88
Slope	1.85	0.54	LST day	1.59	0.63
Aspect	1.02	0.98	LST night	1.18	0.84
TWI	1.34	0.74	Distance from water bodies	1.23	0.81
Mean temperature	8.30	0.12	Distance from rail	1.23	0.81
Precipitation	1.75	0.57	Distance from road	1.38	0.72
Solar radiation	2.33	0.43	Distance from settlement	1.29	0.77
Wind speed	1.25	0.80	Forest type	1.68	0.60
NDVI	6.63	0.15	NDWI	5.33	0.19

The variable layers for all the above-mentioned variables enlisted in Table 1 are shown below (Figure 3). The layers were reclassified into five classes manually on the basis of distribution of pixel and past fire incidences within the study sites explained in Table 2.

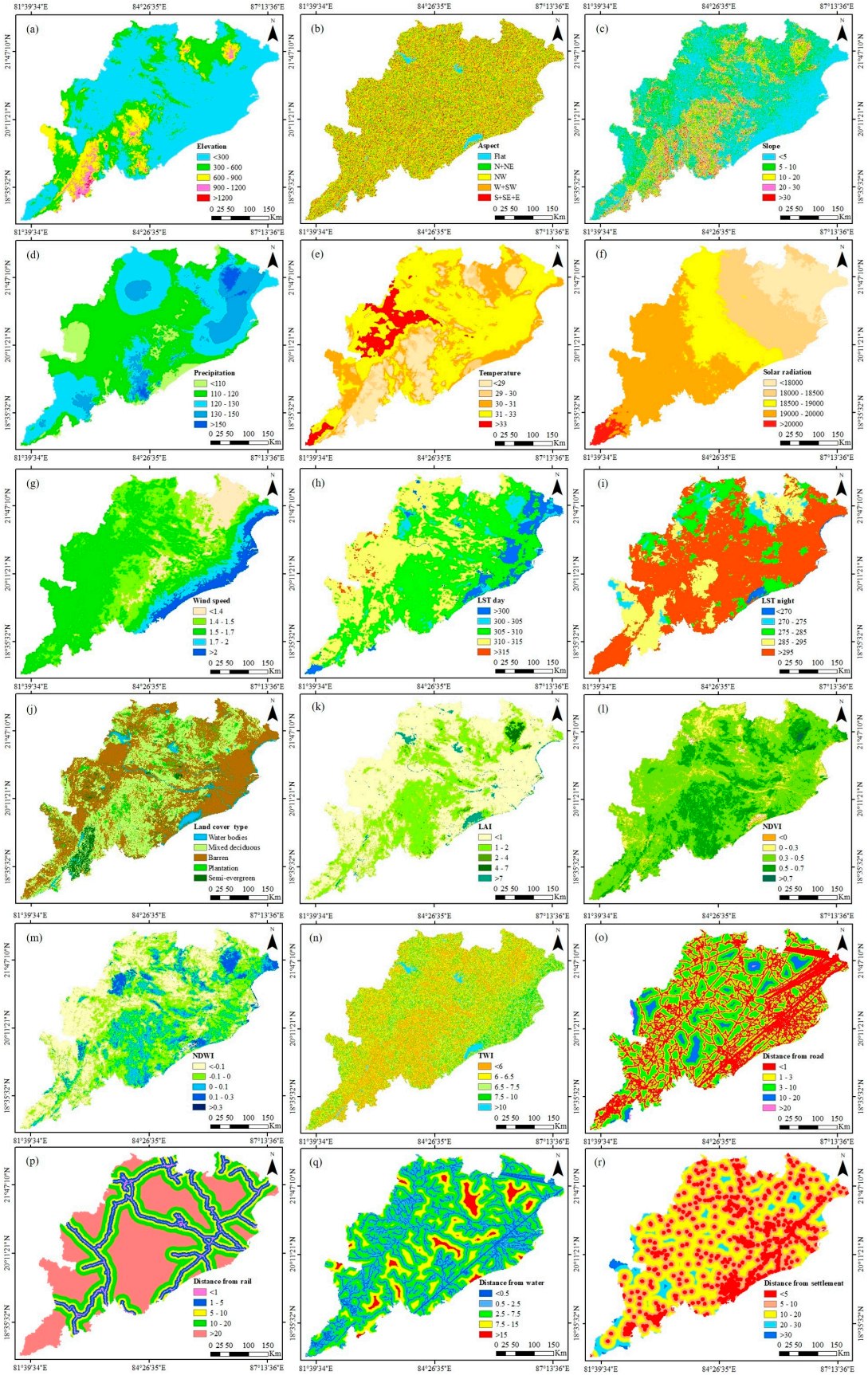

Figure 3. Thematic map of responsible variable layers (a–r).

Table 2. Selected variables class distribution details.

Variables	Classes Distribution
Elevation (Figure 3a)	<300, 300–600, 600–900, 900–1200, and >1200 (in m)
Aspect (Figure 3b)	Flat, North and Northeast (N + NE), Northwest (NW), West and Southwest (W + SW), and South, Southeast and East (S + SE + E)
Slope angle (Figure 3c)	<5, 5–10, 10–20, 20–30, and >30 (in °)
Precipitation (Figure 3d)	<110, 110–120, 120–130, 130–150, and >150 (in mm)
Temperature (Figure 3e)	<29, 29–30, 30–31, 31–33, and >33 (in °C)
Solar radiation (Figure 3f)	<18,000, 18,000–18,500, 18,500–19,000, 19,000–20,000, and >20,000 (in $kJm^{-2}day^{-1}$)
Wind speed (Figure 3g)	<1.4, 1.4–1.5, 1.5–1.7, 1.7–2.0, and >2.0 (in ms^{-1})
LST day (Figure 3h)	<300, 300–305, 305–310, 310–315, and >315 (in K)
LST night (Figure 3i)	<270, 270–275, 275–285, 285–295, and >295 (in K)
Land cover type (Figure 3j)	Mixed deciduous, Semi-evergreen, Plantation, Barren, and Water bodies
LAI (Figure 3k)	<1, 1–2, 2–4, 4–7, and >7
NDVI (Figure 3l)	<0, 0–0.3, 0.3–0.5, 0.5–0.7, and >0.7
NDWI (Figure 3m)	<−0.1, −0.1–0, 0–0.1, 0.1–0.3, and >0.3
TWI (Figure 3n)	<6, 6–6.5, 6.5–7.5, 7.5–10, and >10
Distance from road (Figure 3o)	<1, 1–3, 3–10, 10–20, and >20 (in km)
Distance from rail (Figure 3p)	<1, 1–5, 5–10, 10–20, and >20 (in km)
Distance from water bodies (Figure 3q)	<0.5, 0.5–2.5, 2.5–7.5, 7.5–15, and >15 (in km)
Distance from settlement (Figure 3r)	<5, 5–10, 10–20, 20–30, >30 (in km)

2.5. Model Description

2.5.1. Frequency Ratio (FR)

The FR method is an empirical approach as it does not depend on statistical distribution [33,34]. It displays correlation between past incident locations and variables contributing occurrence of hazard in the area on the basis of association between them [35]. FR is explained as ratio of the area where forest fire occurred in the total study area. It is calculated as the probability between occurrences and absences of forest fire within variable classes. The FR value for each class within the variables were calculated (Table 3) and final values were summed up to generate the Forest Fire Susceptibility Index (FFSI). The value equal to 1 indicates as average value while the value <1 is considered as lower correlation, whereas value >1 means higher correlation [33,35].

$$\boldsymbol{FFSI = Fr_1 + Fr_2 + Fr_3 + \ldots\ldots + Fr_n} \quad (1)$$

where Fr is the rating of each variable range.

Table 3. Classification of variables and weights computed to generate forest fire susceptibility map.

Sl No	Parameter	Classes	Firepoint	% Firepoint	No. of Pixel	% Pixel	FR	NRF	W	CF	Wi	Wf	AHP	
1	Elevation	<300	6641	21.054	10,081,077	13.843	1.521	1.053	1	0.343	0.419	100	0.058	
		300–600	10,432	33.072	38,030,875	52.222	0.633	1.654	1	−0.367	−0.457		0.236	λ_{max} = 5.306
		600–900	11,819	37.469	20,178,724	27.708	1.352	1.873	1	0.261	0.302		0.536	CI = 0.076
		900–1200	2506	7.945	4,306,390	5.913	1.344	0.397	0	0.256	0.295		0.134	
		>1200	145	0.460	228,998	0.314	1.462	0.023	0	0.316	0.380		0.035	CR = 0.069
2	Aspect	Flat	14	0.044	2,333,606	12.644	0.004	0.002	0	−0.996	−5.652	1	0.041	λ_{max} = 5.283
		N + NE	7497	23.768	4,208,371	22.802	1.042	1.188	1	0.041	0.041		0.051	
		NW	12,336	39.109	6,098,469	33.044	1.184	1.955	1	0.155	0.169		0.292	CI = 0.071
		W + SW	7797	24.719	3,837,835	20.795	1.189	1.236	1	0.159	0.173		0.498	
		S + SE + E	3899	12.361	1,977,539	10.715	1.154	0.618	0	0.133	0.143		0.117	CR = 0.064
3	Slope	<5	5649	17.909	8,043,419	42.239	0.424	0.895	0	−0.576	−0.858	89.792	0.060	λ_{max} = 5.198
		5–10	6889	21.840	4,270,390	22.425	0.974	1.092	1	−0.027	−0.026		0.125	
		10–20	10,413	33.012	2,605,392	13.682	2.413	1.651	1	0.587	0.881		0.309	CI = 0.049
		20–30	6656	21.101	1,137,790	5.975	3.532	1.055	1	0.718	1.262		0.469	
		>30	1936	6.138	2,985,836	15.680	0.391	0.307	0	−0.609	−0.938		0.037	CR = 0.045
4	Temperature	<29	13,965	44.273	22,878	12.611	3.511	2.214	2	0.866	1.256	52.125	0.519	λ_{max} = 5.175
		29–30	6125	19.418	16,332	9.002	2.157	0.971	0	0.649	0.769		0.143	
		30–31	5399	17.116	35,584	19.614	0.873	0.856	0	−0.150	−0.136		0.068	CI = 0.044
		31–33	5919	18.765	93,268	51.410	0.365	0.938	0	−0.678	−1.008		0.033	
		>33	135	0.428	13,357	7.363	0.058	0.021	0	−0.951	−2.845		0.237	CR = 0.039
5	Precipitation	<110	1889	5.989	14,886	8.205	0.730	0.299	0	−0.309	−0.315	92.462	0.034	λ_{max} = 5.119
		110–120	14,210	45.050	78,272	43.144	1.044	2.252	2	0.051	0.043		0.285	
		120–130	9387	29.759	60,623	33.416	0.891	1.488	1	−0.129	−0.116		0.134	CI = 0.029
		130–150	4952	15.699	24,548	13.531	1.160	0.785	0	0.167	0.149		0.078	
		>150	1105	3.503	3090	1.703	2.057	0.175	0	0.622	0.721		0.468	CR = 0.027

Table 3. *Cont.*

Sl No	Parameter	Classes	Firepoint	% Firepoint	No. of Pixel	% Pixel	FR	NRF	W	CF	Wi	Wf	AHP	
6	Solar radiation	<18,000	1907	6.046	24,140	13.306	0.454	0.302	0	−0.592	−0.789	51.319	0.038	λ_{max} = 5.283
		18,000–18,500	2956	9.371	42,806	23.595	0.397	0.469	0	−0.648	−0.923		0.073	
		18,500–19,000	7127	22.595	40,741	22.457	1.006	1.130	1	0.007	0.006		0.409	CI = 0.071
		19,000–20,000	19,263	61.069	70,150	38.667	1.579	3.053	2	0.444	0.457		0.367	
		>20,000	290	0.919	3582	1.974	0.466	0.046	0	−0.581	−0.764		0.114	CR = 0.064
7	Wind speed	<1.4	3352	10.627	19,992	11.020	0.964	0.531	0	−0.043	−0.036	31.962	0.513	λ_{max} = 5.102
		1.4–1.5	14,461	45.845	53,611	29.551	1.551	2.292	2	0.430	0.439		0.238	
		1.5–1.7	12,821	40.646	84,344	46.491	0.874	2.032	2	−0.148	−0.134		0.151	CI = 0.025
		1.7–2	729	2.311	12,134	6.688	0.346	0.116	0	−0.696	−1.063		0.061	
		>2	180	0.571	11,338	6.250	0.091	0.029	0	−0.923	−2.394		0.037	CR = 0.023
8	LSTday	<300	543	1.721	8791	7.926	0.217	0.086	0	−0.834	−1.527	46.849	0.036	λ_{max} = 5.332
		300–305	1698	5.383	5460	4.923	1.094	0.269	0	0.119	0.089		0.529	
		305–310	23,617	74.872	52,544	47.374	1.580	3.744	2	0.513	0.458		0.229	CI = 0.083
		310–315	5549	17.592	43,323	39.061	0.450	0.880	0	−0.630	−0.798		0.129	
		>315	136	0.431	794	0.716	0.602	0.022	0	−0.480	−0.507		0.077	CR = 0.075
9	LSTnight	<270	10	0.032	1052	0.948	0.033	0.002	0	−0.976	−3.398	20.668	0.035	λ_{max} = 5.257
		270–275	998	3.164	4605	4.152	0.762	0.158	0	−0.304	−0.272		0.061	
		275–285	2432	7.710	14,873	13.410	0.575	0.386	0	−0.508	−0.553		0.140	CI = 0.064
		285–295	8512	26.985	20,885	18.830	1.433	1.349	1	0.422	0.360		0.283	
		>295	19,591	62.109	69,497	62.660	0.991	3.105	2	−0.012	−0.009		0.480	CR = 0.058
10	Land cover type	Mixed deciduous	24,355	77.212	9,822,1091	66.037	1.169	3.861	2	0.145	0.156	35.210	0.262	λ_{max} = 5.175
		Semi-evergreen	298	0.945	11,330,787	7.618	0.124	0.047	0	−0.876	−2.087		0.060	
		Plantation	2567	8.138	12,459,729	8.377	0.971	0.407	0	−0.029	−0.029		0.139	CI = 0.044
		Barren	3525	11.175	15,165,589	10.196	1.096	0.559	0	0.088	0.092		0.500	
		Riverine	798	2.530	11,560,215	7.772	0.326	0.126	0	−0.675	−1.122		0.038	CR = 0.039
11	LAI	<1	7704	24.424	455,128	65.010	0.376	1.221	1	−0.635	−0.979	32.024	0.243	λ_{max} = 5.195
		1–2	22,791	72.254	214,892	30.695	2.354	3.613	2	0.602	0.856		0.523	
		2–4	759	2.406	7061	1.009	2.386	0.120	0	0.608	0.870		0.066	CI = 0.049
		4–7	273	0.865	6733	0.962	0.900	0.043	0	−0.104	−0.105		0.127	
		>7	16	0.051	16,277	2.325	0.022	0.003	0	−0.979	−3.825		0.041	CR = 0.044

Table 3. *Cont.*

Sl No	Parameter	Classes	Firepoint	% Firepoint	No. of Pixel	% Pixel	FR	NRF	W	CF	Wi	Wf	AHP	
12	NDVI	<0	0	0.000	2148	0.489	0.000	0.000	0	−1.000	0.000	55.701	0.035	λ_{max} = 5.266
		0–0.3	600	1.902	41,631	9.477	0.201	0.095	0	−0.811	−1.606		0.062	
		0.3–0.5	13,506	42.818	294,447	67.031	0.639	2.141	2	−0.379	−0.448		0.106	CI = 0.067
		0.5–0.7	17,349	55.001	98,838	22.501	2.444	2.750	2	0.637	0.894		0.284	
		>0.7	88	0.279	2205	0.502	0.556	0.014	0	−0.861	−0.587		0.514	CR = 0.059
13	NDWI	<−0.1	5197	16.476	160,255	36.477	0.452	0.824	0	−0.567	−0.795	82.438	0.060	λ_{max} = 5.305
		−0.1–0	14,963	47.437	185,886	42.312	1.121	2.372	2	0.116	0.114		0.321	
		0–0.1	9967	31.598	70,653	16.082	1.965	1.580	1	0.529	0.675		0.110	CI = 0.076
		0.1–0.3	1416	4.489	22,255	5.066	0.886	0.224	0	−0.122	−0.121		0.477	
		>0.3	0	0.000	278	0.063	0.000	0.000	0	−1.000	0.000		0.032	CR = 0.069
14	TWI	<6	15,921	50.474	5,108,265	21.454	2.353	2.524	2	0.576	0.856	61.947	0.497	λ_{max} = 5.138
		6–6.5	4849	15.373	3,062,640	12.863	1.195	0.769	0	0.163	0.178		0.254	
		6.5–7.5	5582	17.696	4,175,465	17.537	1.009	0.885	0	0.009	0.009		0.155	CI = 0.034
		7.5–10	4205	13.331	3,180,920	13.360	0.998	0.667	0	−0.002	−0.002		0.060	
		>10	986	3.126	8,282,846	34.787	0.090	0.156	0	−0.910	−2.410		0.034	CR = 0.031
15	Distance from road	<1	5145	16.311	6,006,263	26.090	0.625	0.816	0	−0.375	−0.470	71.739	0.510	λ_{max} = 5.237
		1–3	8058	25.546	5,112,878	22.209	1.150	1.277	1	0.131	0.140		0.264	
		3–10	14,036	44.498	4,520,205	19.635	2.266	2.225	2	0.560	0.818		0.130	CI = 0.059
		10–20	4089	12.963	7,150,172	31.059	0.417	0.648	0	−0.583	−0.874		0.064	
		>20	215	0.682	231,630	1.006	0.677	0.034	0	−0.323	−0.389		0.033	CR = 0.053
16	Distance from rail	<1	426	1.351	6,494,457	29.225	0.046	0.068	0	−0.954	−3.075	35.398	0.510	λ_{max} = 5.237
		1–5	1895	6.008	2,219,039	9.986	0.602	0.300	0	−0.399	−0.508		0.264	
		5–10	3018	9.568	2,391,306	10.761	0.889	0.478	0	−0.111	−0.117		0.130	CI = 0.059
		10–20	5612	17.792	3,824,770	17.211	1.034	0.890	0	0.033	0.033		0.064	
		>20	20,592	65.282	7,292,978	32.818	1.989	3.264	2	0.498	0.688		0.033	CR = 0.053

Table 3. *Cont.*

Sl No	Parameter	Classes	Firepoint	% Firepoint	No. of Pixel	% Pixel	FR	NRF	W	CF	Wi	Wf	AHP	
17	Distance from water bodies	<0.5	1534	4.863	1,812,501	8.558	0.568	0.243	0	−0.432	−0.565	61.319	0.036	λ_{max} = 5.265
		0.5–2.5	6138	19.459	4,745,758	22.409	0.868	0.973	0	−0.132	−0.141		0.102	
		2.5–7.5	13,935	44.178	6,303,685	29.765	1.484	2.209	2	0.327	0.395		0.268	CI = 0.066
		7.5–15	8557	27.128	2,982,205	14.082	1.926	1.356	1	0.482	0.656		0.538	
		>15	1379	4.372	5,333,884	25.186	0.174	0.219	0	−0.827	−1.751		0.056	CR = 0.059
18	Distance from settlement	<5	4674	14.818	3,985,083	15.709	0.943	0.741	0	−0.057	−0.058	52.717	0.510	λ_{max} = 5.237
		5–10	8770	27.803	5,615,606	22.136	1.256	1.390	1	0.204	0.228		0.264	
		10–20	14,964	47.440	5,777,885	22.776	2.083	2.372	2	0.521	0.734		0.130	CI = 0.059
		20–30	2840	9.004	8,963,108	35.332	0.255	0.450	0	−0.745	−1.367		0.064	
		>30	295	0.935	1,026,536	4.047	0.231	0.047	0	−0.769	−1.465		0.033	CR = 0.053

2.5.2. Certainty Factor (CF)

The CF method is a probability function approach, applied to determine spatial relationship between fire points in the study site with each variable [36]. It was originally applied by Shortliffe et al. [37] and later modified by Heckerman [38], calculated for each class of all variables is as follows:

$$CF_{ia} = \begin{cases} pp_{ia} - pp_f/pp_{ia}(1 - pp_f), & if\ pp_{ia} \geq pp_f \\ pp_{ia} - pp_f/pp_f(1 - pp_{ia}), & if\ pp_{ia} < pp_f \end{cases} \quad (2)$$

where CF_{ia} is the Certainty factor of certain class i of variable a; pp_{ia} is the conditional probability of having number of forest fire occurring in a class i of variable a; and pp_f is the prior probability of having the total number of forest fire occurring in the study area.

Its value ranges between −1 and 1. The negative CF value directs least chance of forest fire in the site, while the positive value indicates high susceptibility, and value near to 0 specify prior probability is equal to conditional probability [33]. Thus, site with zero CF value indicates inadequate relationship between fire and responsible variables, making difficult to infer certainty of fire in those forest patches [36]. After calculating the CF value for each class of variable layer (Table 3), the layers were integrated using the rule of X:

$$X = \begin{cases} CF_A + CF_B - CF_A CF_B & CF_A, CF_B \geq 0 \\ \dfrac{CF_A + CF_B}{1 - min(|CF_A|, |CF_B|)} & CF_A, CF_B\ opposite\ sign \\ CF_A + CF_B + CF_A CF_B & CF_A, CF_B < 0 \end{cases} \quad (3)$$

where CF_A and CF_B are CF values of A and B variable layers, respectively. The pairwise addition was done until all responsible layers were summed up to produce final forest fire susceptibility map.

2.5.3. Bivariate Statistical Method (W_i and W_f)

The statistical index (W_i) method [39], and the weighting factor (W_f) method [40] was used to analyze occurrence of forest fire in the study site. W_i is based on statistical correlation of fire inventory map with variable layers. The result provides density of fire hazard in each variable class. The W_i value for each class was calculated using the formula given by [39]:

$$W_i = \ln \frac{\text{Density class}}{\text{Density map}} = \ln \frac{\frac{N_x}{C_{pix}}}{\frac{TN_x}{TC_{pix}}} \quad (4)$$

where W_i is the weight given to specified class, **Density class** is the forest fire density within variable class, **Density map** is the forest fire density within study area, N_x is the fire point within a specified variable class, C_{pix} is the number of pixels in certain variable class, TN_x is the total number of fire points in the study area, and TC_{pix} is the total number of pixels in the study area.

The W_i value for each variable class was calculated (Table 3). Finally, all variable layers were overlaid to generate the fire susceptibility map. The weighting factor (W_f) was computed for each variable map to eliminate consideration of equal effect of each variable layer while using the statistical method in predicting W_i value, which may not be in natural condition [35]. For calculating W_f, the W_i, value of each pixel was calculated, then pixels within high fire susceptibility zones of each variable layer were summed. The outcomes were distorted by employing the highest and the lowest layer values. Finally, the formula shown below was used to calculate the weighting factor, which ranges from 1 to 100 for each layer:

$$W_f = \frac{(Total\ Wi_{value}) - (MinTotal\ Wi_{value})}{(MaxTotal\ Wi_{value}) - (MinTotal\ Wi_{value})} \times 100 \quad (5)$$

where $\boldsymbol{Total\ Wi_{value}}$ is the total $\boldsymbol{W_i}$ value of pixels within forest fire zone for each variable, $\boldsymbol{MinTotal\ Wi_{value}}$ is the minimum total $\boldsymbol{W_i}$ value within selected layers, and $\boldsymbol{MaxTotal\ Wi_{value}}$ is the maximum total $\boldsymbol{W_i}$ value within selected layers.

The $\boldsymbol{W_f}$ values of each variable layer were calculated (Table 3). To generate the final susceptibility map from $\boldsymbol{W_f}$ method, $\boldsymbol{W_f}$ value of each layer was multiplied by $\boldsymbol{W_i}$ value of each variable class.

2.5.4. Natural Risk Factor (NRF)

NRF is a problem-solving approach, which used the weighted method of analysis. The weight (W) for each variable assigned using the ratio of proportion of fire occurrences in a specified class and average occurrences in all classes [41]. The weights calculated in Table 3 were assigned to each pixel of the variable layers. The classes with proportion <1 have weights 0, for proportion 1<–<2 is 1 and 2 for proportion >2. After assigning of weights to pixels of each variable, a fire susceptibility map was generated by adding values of each pixel [34].

2.5.5. Analytical Hierarchy Process (AHP)

AHP developed by Saatty [42], is a multi-criteria decision-making approach providing technique for structuring and analyzing complex decisions. It makes the decision-making process transparent and simpler to arrive at a preference from a set of alternatives through pairwise comparison matrix of criteria [18]. The variable layers were categorized into criteria and variable classes as set of alternatives. The relative importance value (1–9) to each variable class for its contribution towards forest fire occurrence was assigned according to expert opinion and literature. The score for each layer was computed from the relative importance value assigned to each variable class through calculation of matrix eigenvalues. To validate the pairwise decision matrix formed, consistency ratio (CR) was calculated which should be less than 10% (0.1), computed by

$$\boldsymbol{CR = CI/RI} \tag{6}$$

where $\boldsymbol{CI}$ is consistency index, $\boldsymbol{RI}$ is the average of the resulting consistency index depending on the order of the matrix.

The $\boldsymbol{CI}$ was computed as followed

$$\boldsymbol{CI = \frac{(\lambda_{max} - n)}{(n - 1)}} \tag{7}$$

where $\boldsymbol{\lambda_{max}}$ is the largest or principal eigenvalue of the matrix and n is order of the matrix.

2.5.6. Logistic Regression (LR)

The LR model or logit model is a statistical method used to model binary dependent variable, i.e., the function is in 0 or 1 [34,43]. It represents the multivariate regression relationship between the given set of responsible variables required to predict fire occurrence [35]. It predicts occurrence or non-occurrence of fire on the basis of set of variables. The variables used for analyzing forest fire in logistic regression may have continuous, discrete or combination of both as data type and do not require normalization, makes it better over linear regression [35]. The influence of each variable on occurrence of forest fire was calculated independently and all the variables were assimilated to form a unique equation [44,45].

$$\boldsymbol{Y = Logit(p) = ln\left(\frac{p}{1 - p}\right)} \tag{8}$$

$$\boldsymbol{Y = C_0 + C_1X_1 + C_2X_2 + \ldots\ldots + C_nX_n} \tag{9}$$

where $\boldsymbol{p}$ is the probability that the dependent variable ($\boldsymbol{Y}$) is 1, $\boldsymbol{\frac{p}{1-p}}$ is the odd or frequency ratio, $\boldsymbol{C_0}$ is the intercept, and $\boldsymbol{C_1, C_2, \ldots\ldots, C_n}$ are the coefficients that measure the contributions of responsible variables ($\boldsymbol{X_1, X_2, \ldots\ldots, X_n}$) to the variations in $\boldsymbol{Y}$.

The spatial association between fire points and responsible variables was evaluated using logistic regression in RStudio environment and the regression equation given below:

Y = 8.1177 + 0.00033 × Aspect − 0.00039 × Elevation − 0.09648 × LAI − 0.00665 × LST day − 0.01005 × LST night + 5.59162 × NDVI − 7.46542 × NDWI − 0.00868 × Precipitation − 0.0000042 × Distance from rail + 0.0000403 × Distance from road + 0.00000367 × Distance from settlement + 0.01231 × Slope angle + 0.00053 × Solar radiation − 0.35696 × Temperature + 0.02653 × TWI − 0.00822 × Land cover type + 0.0000094 × Distance from water bodies − 1.67705 × Wind speed

The regression equation represents aspect, NDVI, distance from road, distance from settlement, slope angle, solar radiation, TWI, and distance from water bodies are positively related to forest fire while elevation, LAI, LST day, LST night, NDWI, precipitation, distance from rail, temperature, land cover type, and wind speed shows negative relation with forest fire. NDVI shows a strong positive relation than other variables used towards forest fire occurrence in the study area.

2.6. Validation and Accuracy Assessment

The next phase of the study includes validation of the six models used for forest fire susceptibility mapping. The area under the receiver operating characteristic curve (ROC curve-AUC value) was used to evaluate goodness-of-fit of the model in correct assessment of occurrence and non-occurrence of forest fire at spatial scale [33,34,46]. It is an effective technique for evaluation of model quality and offer an appealing approach to summarize the precision of prediction accuracy [20]. AUC values range from 0.5 represents a random prediction to 1 as better performance [8,46].

3. Results

Forest fire location details were collected from Forest Fire Alerts system 3.0 of the FSI and fire inventory map was prepared. The forest fire events showed a highly increasing rate after 2005. The largest number of fire events were observed in 2017 and 2020 with vast extent of forest patches burnt. March to May had the largest number of fire events while the least fire events were observed in July and August. According to the India Meteorological Department (IMD), Indian climatic season is classified into four seasons: winter, pre-monsoon, monsoon and post-monsoon with the highest fire events of 38,994 in pre-monsoon and the lowest in monsoon of 483.

Natural and anthropogenic causes lead to forest fire. Initiation and spread of fire depend on different variables, which are required to be evaluated for appropriate modelling approach and prediction, so 22 variables were selected from extensive literature. Multicollinearity statistics was used to remove collinear layers using VIF and TOL value (Table 1). Four variables: GPP (28.55), AI (21.51), water vapor pressure (12.63) and PET (11.73), with values of VIF greater than 10 were not used for further modelling. Elevation, slope, aspect, temperature, precipitation, solar radiation, wind speed, NDVI, NDWI, TWI, LST day, LST night, LAI, Land cover type, distance from road, distance from rail, distance from settlement, and distance from water bodies were important variables used for modelling analysis (Figure 3).

Based on weight calculated in Table 3 for elevation, area with <300 m obtained FR = 1.521, and W_i = 0.419 had the greatest effect on fire occurrence while 600–900 m elevation were predicted highly susceptible according to NRF = 1.873 and AHP = 0.536. The CF model ranked higher elevation class (>1200 m) to be highly prone to forest fire occurrence. The models did not show any specific pattern of ranking variable class towards forest fire susceptibility. However, elevation with W_f = 100 indicates the importance of elevation towards occurrence of forest fire. Aspect analysis shows area with West and South west (W + SW) orientations are highly prone to forest fire with FR = 1.189, CF = 0.159, W_i = 0.173, and AHP = 0.498. NRF calculated the highest weights for North-west (NW) orientation is 1.955 followed by W + SW with NRF = 1.236. Slope angle with increasing slope fire susceptibility increases but area with >30°, steep slope, is negatively correlated with fire sus-

ceptibility. Slope from 20° to 30° are calculated with highest weights: FR = 3.532, CF = 0.718, W_i = 1.262, and AHP = 0.469. The LR model predicted that elevation is negatively related while slope and aspect are positively related to forest fire occurrence. The climatic variables including temperature, precipitation, solar radiation and wind speed do not define any specific trend with the weights calculated, but the LR values show positive relationship between solar radiation and negative with wind speed. The areas with temperature <29 °C, the highest precipitation (>150 mm), solar radiation of 19,000–20,000 $kJm^{-2}day^{-1}$, and moderate wind speed of 1.4–1.5 ms^{-1} show higher susceptibility to forest fire. Similarly, LST day with moderate temperature class and LST night with the highest temperature are predicted to be highly contributing to forest fire. Mixed deciduous type is predicted to be highly susceptible to forest fire, followed by semi-evergreen and plantation patches. The climate variables contribute to forest fire occurrence, but key determinants are vegetation [2] and topography [8]. LAI value with 1–2 shows higher susceptibility to forest fire, possibly due to distribution of maximum forest patches within the class in the study area. According to LR model, NDVI shows higher positive relationship with forest fire, while NDWI has negative relationship and similar trend is observed through other five models. Increasing NDVI indicates high susceptibility to forest fire, while inverse relation is showed by NDWI. While TWI also shows an inverse relation with forest fire occurrence, a lower TWI value has a higher chance of fire occurrence and vice-versa, but a positive relationship is predicted according to LR model. Distance from road, rail and settlement show higher forest fire susceptibility with higher Euclidean distance classes and lower for lower distance. This is anticipated that the accessibility of fire-fighting equipment would be related to these two factors since it is frequently transported to the scene by road or rail [12,15]. As a forest patch loses moisture, the susceptibility to forest fire increases with increasing distance from water sources. However, the results of the LR model show that distance from a road, a settlement, and a body of water are all positively related, whereas distance from a railroad is negatively related.

After calculation of the final weights for each variable layer, all the layers were summed up to generate final susceptibility map from six models (Figure 4a–g). The susceptibility maps were classified into five susceptibility classes (very low, low, moderate, high, and very high) using Natural breaks (Jenks) classification scheme. Forest fire points recorded by the MODIS sensor are similar to the distribution pattern of higher susceptibility classes. Fire susceptibility map generated by FR method indicates 26.25%, 30.16%, 18.65%, 14.98% and 9.97% of the total area with very low to very high susceptibility classes, respectively. The CF model defines about 16.29% as very low, 31.29% low, 22.17% moderate, 16.84% high and 13.41% with very high susceptibility. Trend of very low to very high susceptibility classified in the map generated through NRF method is 12.95%, 25.91%, 25.65%, 19.92% and 15.57% of the total area, respectively. The map produced using W_i method comprises very low susceptibility of 1.83% of the total area, low (21.91%), moderate (34.46%), high (23.04%) and very high (18.75%). According to the W_f method about 13.72% area is under very low, 29.4% low, 25.17% moderate, 18.49% high and 13.22% very high susceptibility. About 17.18% area as very low, 28.76% low, 26.1% moderate, 17.8% high and 10.16% very high are categorized according to AHP method. The LR method is able to explain that 14.97% of the total area is very highly susceptible, 29.43% high, 23.33% moderate, 19.7% low and 12.57% with very low susceptibility. On an average around 25–35% of the study area are marked under high to very high susceptibility, which prioritize the need of fire management plan. The southern tip of Odisha lies in very high susceptibility, while coastal zone and urbanized area are under the least susceptibility.

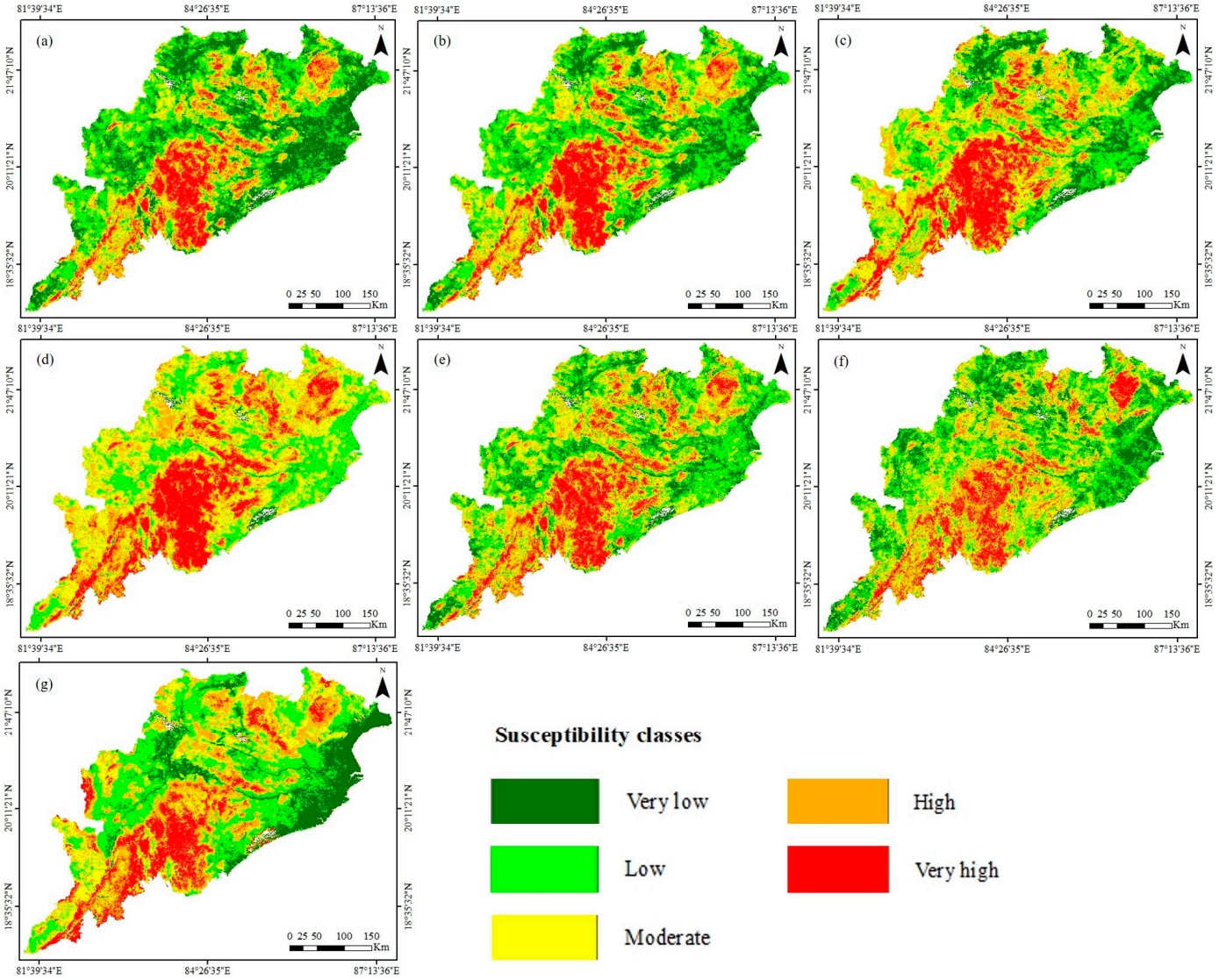

Figure 4. Forest fire susceptibility maps using (**a**) FR, (**b**) CF, (**c**) NRF, (**d**) W_i, (**e**) W_f, (**f**) AHP, and (**g**) LR.

The final phase of the study comprises of validation of models. According to the defined methodology, prediction curve for each model was validated using AUC value. Figure 5 shows ROC curve and AUC value of each model used in the study. LR model showed the highest AUC value of 80% with better prediction value and conclude good fit of model. While other models have AUC value more than 75% showing good fit of model in prediction of forest fire susceptibility for the study area.

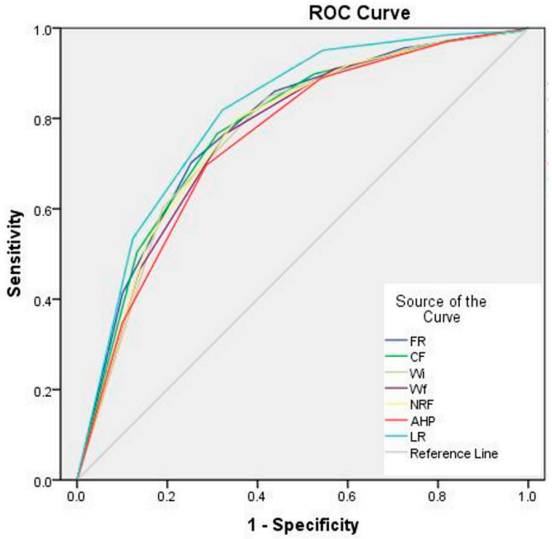

Area Under the Curve

Test Result Variable(s)	Area	Std. Error[a]	Asymptotic Sig.[b]	Asymptotic 95% Confidence Interval	
				Lower Bound	Upper Bound
FR	0.779	0.003	0.000	0.774	0.784
CF	0.778	0.003	0.000	0.772	0.783
Wi	0.766	0.003	0.000	0.761	0.772
Wf	0.764	0.003	0.000	0.758	0.769
NRF	0.769	0.003	0.000	0.763	0.774
AHP	0.753	0.003	0.000	0.748	0.759
LR	0.809	0.003	0.000	0.804	0.814

The test result variable(s): FR, CF, Wi, Wf, NRF, AHP, LR has at least one tie between the positive actual state group and the negative actual state group. Statistics may be biased.

a. Under the nonparametric assumption

b. Null hypothesis: true area = 0.5

Figure 5. ROC and AUC value of models predicted used for validation.

4. Discussion

For effective fire risk management, it is crucial to provide a high-quality map of the susceptibility of forest fires [11,47,48]. However, this effort is still challenging because of how complicated and non-linear such events are. To get a trustworthy assessment of their occurrence risk, using optimization approaches appears to be an intellectual problem [49]. This paper investigated the comparative effect of environmental variable classes on fire zones with weighted modelling and how forest fire susceptible maps could be used for fire management. Topography shows effect on fire by influencing vegetation, local climate, ignition pattern and accessibility to humans [8,50]. Topography indirectly affects flammability in a forest [12,51], as it determines distribution of vegetation pattern and composition, and influences climatic factors [33,52]. Slope acts as a key restricting factor to ignition by limiting accessibility because anthropogenic fire occurs more frequently in gentler slopes [12]. Topography explains a site condition with variables like elevation range, angle of slope, land facing towards sun (aspect) and water retention ability by the landscape [53,54].

Vegetation type is the most significant explaining ignition of forest fires [5]. Biophysical component makes conditions suitable for forest fire occurrence. Positive feedback mechanism between vegetation and fire spread and intensity make tropical forests prone to degradation [10,55]. The NDVI describes forest health condition, which gives an idea of fuel load distribution and its deposition [33]. Studies inferred biophysical factors like GPP, NDWI, LAI, LST, PET, and AI also make up conditions favorable for wildfire [30,56,57]. The climate conditions with reduced rainfall and vapor pressure, increasing temperature, humidity and solar radiation contribute towards the occurrence of forest fire. Climate largely contributes to nature of wildfire and describes the need of changing fire management practices with spatial and temporal variations, so that it is considered as a major component of fire environment [23,58]. Climate directs fuel characterization like fuel load, moisture content, degradation which regulate proneness of regional forest to fire [14,25].

With the above all supporting variables uncontrolled and careless human activities further provoke chance of fire occurrence and major contributor towards susceptibility of a site [14,59]. Anthropogenic interference regulates forest fire frequency and spread [3] by providing ignition source and changing vegetation type, which may either limit or promote forest fire [8]. It is vital to consider societal conditions in forest fire susceptibility mapping. Spatial proximity to growing settlement specifies intensity of disturbances in forest [60,61]. Construction activities like roads and railways increase accessibility leading to higher probability of fire incidences [10], while presence of water bodies acts as a natural suppressor of fire.

In order to control risk and avoid fires in the research region, the susceptibility maps can be utilised as a reference. They were created by using modelling approach and GIS dataset. Six models were used in this study to investigate the geographical association between fire responsible variables and fire events. Based on the distribution of pixels and historical fire occurrences within the research locations, the variables were manually categorized into five groups. According to the study, Wi shows that close to 42% of the region is in the "high to very high susceptibility class," while FR, CF, NRF, Wf, AHP, and LR methods demarcate roughly 25–35% of the entire area. For anticipating unforeseen forest fire occurrences, the LR model of susceptibility demonstrated great accuracy (80%). The majority of the stretch with tropical deciduous forest having tribal dominating population, found to be highly prone to forest fires.

It is critical to take necessary precautions to reduce the likelihood of this environmental catastrophe, since according to some local sources, human factors—such as tourists and travellers—were mostly to blame for the recent fires. Abedi Gheshlaghi et al. and Divya et al. [60,62] found that using several well-known land management techniques like controlled burn approach in highly sensitive places can significantly lower the risk. Another viable strategy for preventing future fires in the study area is use of various forest fire early warning systems [22,63,64]. The Government of India has created the National Action Plan on Forest Fires, 2018, to prevent forest fires by empowering communities that border forests, and motivating them to collaborate with the State Forest Departments.

It is important to remember that using the models suggested in the current study have their limits. Most significantly, the models may not be as accurate as they are in the presence of significant changes in variable components since they were constructed using geo-environmental data from a given time period (e.g., precipitation, LST). Such circumstances require periodic updating of the produced susceptibility maps. Another issue was the lack of information on the precise causes of the fires. It would have been more intriguing to look into the causes of subsequent fire incidents. Furthermore, the created models are very complicated as a result of the vast dimensions (i.e., 18 individual parameters), which is represented by the lengthy computation time of the models (by comparison). However, this flaw may be overcome by improving the input configuration, which is a strong notion for further research.

Recommending Forest Fire Management

A complicated and hazardous environmental occurrence, forest fires or wildfires may occur everywhere in the world as a result of both natural and manmade activities [65–67]. Due to high temperatures and pockets of deciduous forest, the month of February through the month of May in India is particularly prone to forest fires [68]. Numerous studies have shown that anthropogenic factors, such as gathering non-timber forest products, burning farm waste, throwing burning cigarettes or bidis, starting campfires, cooking close-by forests, and sparks from transformers, among others, play a significant role, especially in tropical and subtropical regions of the world. The natural causes of forest fires, such as lightning, rolling stones, rubbing of dry long trees, particularly bamboos, and rolling of dry rocks, are the main causes of forest fires [69]. The focus of several pertinent management strategies has been on preventing the environmental hazard or disaster. The government should construct instruments that enable decision-making, like as monitoring stations, patrol routes along forest buffers, firefighting equipment, fire distinguishing chemicals, etc. Emergency services should be made available and ready by the forest department. The government should implement strict laws and regulations to limit illegal animal hunting and poaching, forbid campfires and picnics inside of forests, control Jhum or shifting cultivation, especially in North East India, continuously monitor forest dwellers and people who live near forests while collecting non-timber forest products, outlaw burning and cooking near forests, forbid matchboxes and bidis in forests, and do not allow the use of firearms or fireworks inside of forests. Governmental and non-governmental groups should educate forest inhabitants, residents on the forest periphery, and visitors about

environmental issues. The importance of wild animals, forest resources, and other things should be made known to the public. The forest department should create artificial forests or reforest the forest buffer and implement joint forest management (JFM) strategies, as well as programs to increase the ability of forest residents and lessen their reliance on the natural world. Similar to this, the government should support academic and scientific applied research into forest fires in order to enhance the standard of living for those who live in and around forests.

5. Conclusions

Forest fire susceptibility prediction using the statistical model is helpful to order which areas of the study area are very high susceptible. In this research, modelling results demarcate southern tip of the state lying in the Eastern Ghats region is more prone to fire. This may be due to the predominance of forest cover in these regions providing ample litter supply, in addition to elevation acts an important promoter of forest fires in these areas. Fire responsible variables and post events were used for modelling and LR model proved to be the best. It would help in understanding extreme ecological approaches, aiding the monitoring of forest remnants of tropical forests. Modeling and mapping of fire susceptibility analysis aid in monitoring hotspot proneness, enable robust control with optimal resource utilization, effective and timely evaluation of associated danger, and development of better fire-fighting strategies. Arson fire events could be reduced with community participation in knowledge-driven programs and conservation activities. Construction of a fire line and ongoing maintenance of it in high susceptibility area can lessen conflagration during hotter and drier seasons.

Author Contributions: The authors confirm contribution to the paper as follows: study conception and design: J.D. and P.K.J.; data collection: J.D.; analysis and interpretation of results: J.D. and P.K.J.; draft manuscript preparation: J.D., S.M., P.K.J. and Y.-A.L.; reviewing and editing: S.M., P.K.J. and Y.-A.L. All authors have read and agreed to the published version of the manuscript.

Funding: This research is funded by Taiwan National Science and Technology Council (NSTC) under project codes: 108-2923-M-008-002-MY3 and 110-2634-F-008-008.

Data Availability Statement: Data will be made available on reasonable request.

Acknowledgments: The authors are thankful to USGS Earth Explorer, Worldclim, CIGAR-GIS, and OSM for providing dataset free of cost. JD acknowledge UGC for providing support to conduct this study. The authors are grateful to anonymous reviewers and editorial board for their constructive comments which led to improvement of this manuscript presentation.

Conflicts of Interest: The authors declare no conflict of interest.

References

1. Feurdean, A.; Veski, S.; Florescu, G.; Vannière, B.; Pfeiffer, M.; O'Hara, R.B.; Stivrins, N.; Amon, L.; Heinsalu, A.; Vassiljev, J.; et al. Broadleaf deciduous forest counterbalanced the direct effect of climate on Holocene fire regime in hemiboreal/boreal region (NE Europe). *Quat. Sci. Rev.* **2017**, *169*, 378–390. [CrossRef]
2. Naderpour, M.; Rizeei, H.M.; Khakzad, N.; Pradhan, B. Forest fire induced Natech risk assessment: A survey of geospatial technologies. *Reliab. Eng. Syst. Saf.* **2019**, *191*, 106558. [CrossRef]
3. Eskandari, S.; Chuvieco, E. Fire danger assessment in Iran based on geospatial information. *Int. J. Appl. Earth Obs. Geoinf.* **2015**, *42*, 57–64. [CrossRef]
4. Tien Bui, D.T.; Bui, Q.T.; Nguyen, Q.P.; Pradhan, B.; Nampak, H.; Trinh, P.T. A hybrid artificial intelligence approach using GIS-based neural-fuzzy inference system and particle swarm optimization for forest fire susceptibility modeling at a tropical area. *Agric. For. Meteorol.* **2017**, *233*, 32–44. [CrossRef]
5. Chitale, V.; Behera, M.D. How will forest fires impact the distribution of endemic plants in the Himalayan biodiversity hotspot? *Biodivers. Conserv.* **2019**, *28*, 2259–2273. [CrossRef]
6. Eskandari, S.; Miesel, J.R. Comparison of the fuzzy AHP method, the spatial correlation method, and the Dong model to predict the fire high-risk areas in Hyrcanian forests of Iran. *Geomat. Nat. Hazards Risk* **2017**, *8*, 933–949. [CrossRef]
7. Tien Bui, D.T.; Le, K.T.T.; Nguyen, V.C.; Le, H.D.; Revhaug, I. Tropical forest fire susceptibility mapping at the Cat Ba National Park area, Hai Phong City, Vietnam, using GIS-based Kernel logistic regression. *Remote Sens.* **2016**, *8*, 347. [CrossRef]

8. Nami, M.H.; Jaafari, A.; Fallah, M.; Nabiuni, S. Spatial prediction of wildfire probability in the Hyrcanian ecoregion using evidential belief function model and GIS. *Int. J. Environ. Sci. Technol.* **2018**, *15*, 373–384. [CrossRef]
9. Mutthulakshmi, K.; Rui, M.; Wee, E.; Chong, Y.; Wong, K.; Cheong, K.H. Simulating forest fire spread and fire-fighting using cellular automata. *Chin. J. Phys.* **2020**, *65*, 642–650. [CrossRef]
10. Murthy, K.K.; Sinha, S.K.; Kaul, R.; Vaidyanathan, S. A fine-scale state-space model to understand drivers of forest fires in the Himalayan foothills. *For. Ecol. Manag.* **2019**, *432*, 902–911. [CrossRef]
11. Ghorbanzadeh, O.; Blaschke, T.; Gholamnia, K.; Aryal, J. Forest fire susceptibility and risk mapping using social/infrastructural vulnerability and environmental variables. *Fire* **2019**, *2*, 50. [CrossRef]
12. Boubeta, M.; Lombardía, M.J.; Marey-Pérez, M.F.; Morales, D. Prediction of forest fires occurrences with area-level Poisson mixed models. *J. Environ. Manag.* **2015**, *154*, 151–158. [CrossRef]
13. Oliveira, S.; Oehler, F.; San-miguel-ayanz, J.; Camia, A.; Pereira, J.M.C. Forest Ecology and Management Modeling spatial patterns of fire occurrence in Mediterranean Europe using Multiple Regression and Random Forest. *For. Ecol. Manag.* **2012**, *275*, 117–129. [CrossRef]
14. Duarte, L.; Teododo, A.C. An easy, accurate and efficient procedure to create forest fire risk maps using the SEXTANTE plugin Modeler. *J. For. Res.* **2016**, *27*, 1361–1372. [CrossRef]
15. Alcasena, F.J.; Ager, A.A.; Salis, M.; Day, M.A.; Vega-Garcia, C. Optimizing prescribed fire allocation for managing fire risk in central Catalonia. *Sci. Total Environ.* **2018**, *621*, 872–885. [CrossRef]
16. Pourghasemi, H.R.; Beheshtirad, M.; Pradhan, B. A comparative assessment of prediction capabilities of modified analytical hierarchy process (M-AHP) and Mamdani fuzzy logic models using Netcad-GIS for forest fire susceptibility mapping. *Geomat. Nat. Hazards Risk* **2016**, *7*, 861–885. [CrossRef]
17. Adab, H.; Kanniah, K.D.; Solaimani, K. Modeling forest fire risk in the northeast of Iran using remote sensing and GIS techniques. *Nat. Hazards* **2013**, *65*, 1723–1743. [CrossRef]
18. Eugenio, F.C.; dos Santos, A.R.; Fiedler, N.C.; Ribeiro, G.A.; da Silva, A.G.; dos Santos, Á.B.; Paneto, G.G.; Schettino, V.R. Applying GIS to develop a model for forest fire risk: A case study in Espírito Santo, Brazil. *J. Environ. Manag.* **2016**, *173*, 65–71. [CrossRef]
19. Hong, H.; Tsangaratos, P.; Ilia, I.; Liu, J.; Zhu, A.X.; Xu, C. Applying genetic algorithms to set the optimal combination of forest fire related variables and model forest fire susceptibility based on data mining models. The case of Dayu County, China. *Sci. Total Environ.* **2018**, *630*, 1044–1056. [CrossRef]
20. Gigović, L.; Pourghasemi, H.R.; Drobnjak, S.; Bai, S. Testing a new ensemble model based on SVM and random forest in forest fire susceptibility assessment and its mapping in Serbia's Tara National Park. *Forests* **2019**, *10*, 408. [CrossRef]
21. Abatzoglou, J.T.; Williams, A.P.; Barbero, R. Global emergence of anthropogenic climate change in fire weather indices. *Geophys. Res. Lett.* **2019**, *46*, 326–336. [CrossRef]
22. Barmpoutis, P.; Papaioannou, P.; Dimitropoulos, K.; Grammalidis, N. A review on early forest fire detection systems using optical remote sensing. *Sensors* **2020**, *20*, 6442. [CrossRef]
23. Davis, R.; Yang, Z.; Yost, A.; Belongie, C.; Cohen, W. The normal fire environment—Modeling environmental suitability for large forest wildfires using past, present, and future climate normals. *For. Ecol. Manag.* **2017**, *390*, 173–186. [CrossRef]
24. de Belém Costa Freitas, M.; Xavier, A.; Fragoso, R. Integration of fire risk in a sustainable forest management model. *Forests* **2017**, *8*, 270. [CrossRef]
25. Kerr, G.H.; DeGaetano, A.T.; Stoof, C.R.; Ward, D. Climate change effects on wildland fire risk in the Northeastern and Great Lakes states predicted by a downscaled multi-model ensemble. *Theor. Appl. Climatol.* **2018**, *131*, 625–639. [CrossRef]
26. Fox, D.M.; Martin, N.; Carrega, P.; Andrieu, J.; Adnès, C.; Emsellem, K.; Ganga, O.; Moebius, F.; Tortorollo, N.; Fox, E.A. Increases in fire risk due to warmer summer temperatures and wildland urban interface changes do not necessarily lead to more fires. *Appl. Geogr.* **2015**, *56*, 1–12. [CrossRef]
27. ISFR. *India State of Forest Report*; Forest Survey of India, Ministry of Environment, Forest and Climate Change, Government of India: Dehradun, India, 2021.
28. Champion, H.G.; Seth, S.K. *A Revised Survey of the Forest Types of India*; Manager of Publications, Government of India: Delhi, India, 1968.
29. Pourtaghi, Z.S.; Pourghasemi, H.R.; Rossi, M. Forest fire susceptibility mapping in the Minudasht forests, Golestan province, Iran. *Environ. Earth Sci.* **2015**, *73*, 1515–1533. [CrossRef]
30. Sachdeva, S.; Bhatia, T.; Verma, A.K. GIS-based evolutionary optimized Gradient Boosted Decision Trees for forest fire susceptibility mapping. *Nat. Hazards* **2018**, *92*, 1399–1418. [CrossRef]
31. Pourtaghi, Z.S.; Pourghasemi, H.R.; Aretano, R.; Semeraro, T. Investigation of general indicators influencing on forest fire and its susceptibility modeling using different data mining techniques. *Ecol. Indic.* **2016**, *64*, 72–84. [CrossRef]
32. Tien Bui, D.; Tuan, T.A.; Hoang, N.D.; Thanh, N.Q.; Nguyen, D.B.; Van Liem, N.; Pradhan, B. Spatial prediction of rainfall-induced landslides for the Lao Cai area (Vietnam) using a hybrid intelligent approach of least squares support vector machines inference model and artificial bee colony optimization. *Landslides* **2017**, *14*, 447–458. [CrossRef]
33. Hong, H.; Naghibi, S.A.; Moradi Dashtpagerdi, M.; Pourghasemi, H.R.; Chen, W. A comparative assessment between linear and quadratic discriminant analyses (LDA-QDA) with frequency ratio and weights-of-evidence models for forest fire susceptibility mapping in China. *Arab. J. Geosci.* **2017**, *10*, 167. [CrossRef]

34. Arabameri, A.; Pradhan, B.; Lombardo, L. Comparative assessment using boosted regression trees, binary logistic regression, frequency ratio and numerical risk factor for gully erosion susceptibility modelling. *Catena* **2019**, *183*, 104223. [CrossRef]
35. Yalcin, A.; Reis, S.; Aydinoglu, A.C.; Yomralioglu, T. A GIS-based comparative study of frequency ratio, analytical hierarchy process, bivariate statistics and logistics regression methods for landslide susceptibility mapping in Trabzon, NE Turkey. *Catena* **2011**, *85*, 274–287. [CrossRef]
36. Azareh, A.; Rahmati, O.; Rafiei-Sardooi, E.; Sankey, J.B.; Lee, S.; Shahabi, H.; Ahmad, B.B. Modelling gully-erosion susceptibility in a semi-arid region, Iran: Investigation of applicability of certainty factor and maximum entropy models. *Sci. Total Environ.* **2019**, *655*, 684–696. [CrossRef]
37. Shortliffe, E.H.; Buchanan, B.G. A model of inexact reasoning in medicine. *Math. Biosci.* **1975**, *23*, 351–379. [CrossRef]
38. Heckerman, D. Probabilistic interpretations for MYCIN's certainty factors. *Mach. Intell. Pattern Recognit.* **1986**, *4*, 167–196.
39. van Westen, C.J. Statistical landslide hazard analysis. *Ilwis* **1997**, *2*, 73–84.
40. Cevik, E.; Topal, T. GIS-based landslide susceptibility mapping for a problematic segment of the natural gas pipeline, Hendek (Turkey). *Environ. Geol.* **2003**, *44*, 949–962. [CrossRef]
41. Gupta, R.P.; Joshi, B.C. Landslide hazard zoning using the GIS approach—A case study from the Ramganga catchment, Himalayas. *Eng. Geol.* **1990**, *28*, 119–131. [CrossRef]
42. Saaty, T.L. A scaling method for priorities in hierarchical structures. *J. Math. Psychol.* **1977**, *15*, 234–281. [CrossRef]
43. Lee, S. Application of logistic regression model and its validation for landslide susceptibility mapping using GIS and remote sensing data. *Int. J. Remote Sens.* **2005**, *26*, 1477–1491. [CrossRef]
44. Subedi, P.; Subedi, K.; Thapa, B.; Subedi, P. Sinkhole susceptibility mapping in Marion County, Florida: Evaluation and comparison between analytical hierarchy process and logistic regression based approaches. *Sci. Rep.* **2019**, *9*(1), 7140. [CrossRef] [PubMed]
45. Yesilnacar, E.; Topal, T. Landslide susceptibility mapping: A comparison of logistic regression and neural networks methods in a medium scale study, Hendek region (Turkey). *Eng. Geol.* **2005**, *79*, 251–266. [CrossRef]
46. Chuvieco, E.; Aguado, I.; Yebra, M.; Nieto, H.; Salas, J.; Martín, M.P.; Vilar, L.; Martínez, J.; Martín, S.; Ibarra, P.; et al. Development of a framework for fire risk assessment using remote sensing and geographic information system technologies. *Ecol. Model.* **2010**, *221*, 46–58. [CrossRef]
47. Moayedi, H.; Mehrabi, M.; Bui, D.T.; Pradhan, B.; Foong, L.K. Fuzzy-metaheuristic ensembles for spatial assessment of forest fire susceptibility. *J. Environ. Manag.* **2020**, *260*, 109867. [CrossRef]
48. North, M.P.; Stephens, S.L.; Collins, B.M.; Agee, J.K.; Aplet, G.; Franklin, J.F.; Fule, P.Z. Environmental science. Reform forest fire management. *Science* **2015**, *349*, 1280–1281. [CrossRef]
49. Li, Z.J.; Zhang, K. Comparison of three GIS-based hydrological models. *J. Hydrol. Eng.* **2008**, *13*, 364–370. [CrossRef]
50. Zhang, K.; Ali, A.; Antonarakis, A.; Moghaddam, M.; Saatchi, S.; Tabatabaeenejad, A.; Chen, R.; Jaruwatanadilok, S.; Cuenca, R.; Crow, W.T.; et al. The sensitivity of North American terrestrial carbon fluxes to spatial and temporal variation in soil moisture: An analysis using radar-derived estimates of root-zone soil moisture. *J. Geophys. Res. Biogeosciences* **2019**, *124*, 3208–3231. [CrossRef]
51. Zhao, L.; Du, M.; Du, W.; Guo, J.; Liao, Z.; Kang, X.; Liu, Q. Evaluation of the Carbon Sink Capacity of the Proposed Kunlun Mountain National Park. *Int. J. Environ. Res. Public Health* **2022**, *19*, 9887. [CrossRef]
52. Li, W.; Shi, Y.; Zhu, D.; Wang, W.; Liu, H.; Li, J.; Shi, N.; Ma, L.; Fu, S. Fine root biomass and morphology in a temperate forest are influenced more by the nitrogen treatment approach than the rate. *Ecol. Indic.* **2021**, *130*, 108031. [CrossRef]
53. Liu, Y.; Zhang, K.; Li, Z.; Liu, Z.; Wang, J.; Huang, P. A hybrid runoff generation modelling framework based on spatial combination of three runoff generation schemes for semi-humid and semi-arid watersheds. *J. Hydrol.* **2020**, *590*, 125440. [CrossRef]
54. Zhao, F.; Song, L.; Peng, Z.; Yang, J.; Luan, G.; Chu, C.; Ding, J.; Feng, S.; Jing, Y.; Xie, Z. Night-time light remote sensing mapping: Construction and analysis of ethnic minority development index. *Remote Sens.* **2021**, *13*, 2129. [CrossRef]
55. Li, J.; Wang, Y.; Nguyen, X.; Zhuang, X.; Li, J.; Querol, X.; Li, B.; Moreno, N.; Hoang, V.; Cordoba, P.; et al. First insights into mineralogy, geochemistry, and isotopic signatures of the Upper Triassic high sulfur coals from the Thai Nguyen Coal field, NE Vietnam. *Int. J. Coal Geol.* **2022**, *261*, 104097. [CrossRef]
56. Pan, J.; Wang, W.; Li, J. Building probabilistic models of fire occurrence and fire risk zoning using logistic regression in Shanxi Province, China. *Nat. Hazards* **2016**, *81*, 1879–1899. [CrossRef]
57. Abdollahi, M.; Dewan, A.; Hassan, Q.K. Applicability of remote sensing-based vegetation water content in modeling lightning-caused forest fire occurrences. *ISPRS Int. J. Geo-Inf.* **2019**, *8*, 143. [CrossRef]
58. Xiong, S.; Li, B.; Zhu, S. DCGNN: A single-stage 3D object detection network based on density clustering and graph neural network. *Complex Intell. Syst.* **2022**, 1–10. [CrossRef]
59. Zhang, Y.; Luo, J.; Li, J.; Mao, D.; Zhang, Y.; Huang, Y.; Yang, J. Fast inverse-scattering reconstruction for airborne high-squint radar imagery based on Doppler centroid compensation. *IEEE Trans. Geosci. Remote Sens.* **2021**, *60*, 1–17. [CrossRef]
60. Abedi Gheshlaghi, H.; Feizizadeh, B.; Blaschke, T. GIS-based forest fire risk mapping using the analytical network process and fuzzy logic. *J. Environ. Plan. Manag.* **2019**, *63*, 481–499. [CrossRef]
61. Zhang, K.; Kimball, J.S.; Zhao, M.; Oechel, W.C.; Cassano, J.; Running, S.W. Sensitivity of pan-Arctic terrestrial net primary productivity simulations to daily surface meteorology from NCEP-NCAR and ERA-40 reanalyses. *J. Geophys. Res. Biogeosciences* **2007**, *112*, G01. [CrossRef]

62. Divya, A.; Kavithanjali, T.; Dharshini, P. IoT enabled forest fire detection and early warning system. In Proceedings of the 2019 IEEE International Conference on System, Computation, Automation and Networking (ICSCAN), Pondicherry, India, 29–30 March 2019; pp. 1–5.
63. Nuryanto, D.E.; Pradana, R.P.; Putra, I.D.G.A.; Heriyanto, E.; Linarka, U.A.; Satyaningsih, R.; Hidayanto, N.; Sopaheluwakan, A.; Permana, D.S. Developing models to establish seasonal forest fire early warning system. *IOP Conf. Ser. Earth Environ. Sci.* **2021**, *909*, 012005. [CrossRef]
64. Washaya, P.; Balz, T.; Mohamadi, B. Coherence change-detection with sentinel-1 for natural and anthropogenic disaster monitoring in urban areas. *Remote Sens.* **2018**, *10*, 1026. [CrossRef]
65. Armenteras, D.; Dávalos, L.M.; Barreto, J.S.; Miranda, A.; Hernández-Moreno, A.; Zamorano-Elgueta, C.; González-Delgado, T.M.; Meza-Elizalde, M.C.; Retana, J. Fire-induced loss of the world's most biodiverse forests in Latin America. *Sci. Adv.* **2021**, *7*, 3357. [CrossRef] [PubMed]
66. Senande-Rivera, M.; Insua-Costa, D.; Miguez-Macho, G. Spatial and temporal expansion of global wildland fire activity in response to climate change. *Nat. Commun.* **2022**, *13*, 1208. [CrossRef] [PubMed]
67. Sahana, M.; Ganaie, T.A. GIS-based landscape vulnerability assessment to forest fire susceptibility of Rudraprayag district, Uttarakhand, India. *Environ. Earth Sci.* **2017**, *76*, 1–18. [CrossRef]
68. Satendra; Kaushik, A.D. *Forest Fire Disaster Management*; National Institute of Disaster Management, Ministry of Home Affairs, Government of India: New Delhi, India, 2014.
69. Gupta, B.; Agrawal, G.; Chauhan, A. *Forest Fire: Characteristics and Management*; Studera Press: New Delhi, India, 2022.